

## Preparation, Characterization and Antibacterial Activity of Manganese Oxide Nanoparticles

E. Azhir<sup>a,b</sup>, R. Etefagh<sup>c</sup>, N. Shahtahmasebi<sup>a,b,\*</sup>, M. Mashreghi<sup>b,d</sup> and P. Pordeli<sup>d</sup>

<sup>a</sup>Department of Physics, Ferdowsi University of Mashhad, Mashhad, Iran

<sup>b</sup>Nanoresearch Center, Ferdowsi University of Mashhad, Mashhad, Iran

<sup>c</sup>Department of Physics, Payame Noor University, P. O. BOX 19395-3697, Tehran, Iran

<sup>d</sup>Department of Biology, Faculty of Science, Ferdowsi University of Mashhad, Mashhad, Iran

(Received 3 November 2014, Accepted 23 April 2015)

Manganese oxide nanoparticles (Mn<sub>3</sub>O<sub>4</sub>-NPs) were prepared using precipitation method. The prepared nanoparticles were characterized by a number of techniques, including X-ray diffraction (XRD) analysis, scanning electron microscopy (SEM), transmission electron microscopy (TEM) and Fourier transforms infra red (FT-IR) spectroscopy. The XRD pattern showed that the structure of Mn<sub>3</sub>O<sub>4</sub>-NPs was tetragonal hausmannite. The average particle size, revealed by TEM images, has been about 10-30 nm. The antibacterial activities of various concentrations of Mn<sub>3</sub>O<sub>4</sub>-NPs against human pathogenic bacteria, mainly *Escherichia coli* and *Staphylococcus aureus* have been studied using the Broth Microdilution Method. The antibacterial assay showed that the Mn<sub>3</sub>O<sub>4</sub>-NPs prepared in this work inhibited the growth and multiplication of these tested microorganisms. The results of qualitative antibacterial tests revealed that gram negative bacteria (*E. coli*) were more sensitive to Mn<sub>3</sub>O<sub>4</sub>-NPs than gram positive bacteria (*S. aureus*).

**Keywords:** Mn<sub>3</sub>O<sub>4</sub> nanoparticles, Precipitation method, Antibacterial activity, Broth microdilution method

### INTRODUCTION

In recent years, manganese oxides, due to their electronic and magnetic properties, have attracted considerable scientific and technological attentions [1,2]. It is grown in different kinds of oxides, MnO, Mn<sub>3</sub>O<sub>4</sub>, Mn<sub>2</sub>O<sub>3</sub>, and MnO<sub>2</sub>, due to the presence of three oxidation states of manganese (Mn<sup>2+</sup>, Mn<sup>3+</sup>, and Mn<sup>4+</sup>) [3]. Manganese oxides particularly Mn<sub>3</sub>O<sub>4</sub> Hausmannite are important materials due to their wide range applications, such as high density magnetic, ion-exchange, molecular adsorption, electrochemical, catalysts, and solar energy transformation [4,5]. Mn<sub>3</sub>O<sub>4</sub> has been widely used as the main source of ferrite materials, which have applications in electronic and information technologies [6]. In addition, Mn<sub>3</sub>O<sub>4</sub> is known to be an active catalyst in several oxidations and reductions.

It can be used as a catalyst to limit the emission of NO<sub>x</sub> and CO [7,8]. A number of morphology-controllable synthetic methods for fabrication of Mn<sub>3</sub>O<sub>4</sub> nanostructure have been reported such as reverse micellar precipitation [9], thermal decomposition [10], vapor phase growth [6], reduction and sol-gel processes [5,11].

Over the past few decades, inorganic nanoparticles have attracted a great deal of attention because of their potential for removing environmental pollutants and their antimicrobial properties. Due to the fact that bacteria developed resistance against many common antibacterial agents such as antibiotics, nanomaterials particularly metallic nanoparticles, could open a new avenue in combating dangerous pathogens. Also the majority of researchers perform experiments based on available NPs rather than specific, desired NPs [12]. Mn<sub>3</sub>O<sub>4</sub>-NPs as an effective oxidant have been evaluated for degradation of organic contaminants in water. Antimicrobial properties of

\*Corresponding author. E-mail: nassershah@yahoo.com.au

Mn<sub>3</sub>O<sub>4</sub>-NPs is not well understood and there is just a report on determination the size of inhibition zone diameter when several bacterial species confronted with discs impregnated with the define concentration of Mn<sub>3</sub>O<sub>4</sub> [13]. However, minimum inhibitory concentration (MICs), minimum bactericidal concentration (MBCs) and effect of Mn<sub>3</sub>O<sub>4</sub> on bacterial growth are still under question.

In this paper, nanoparticles of Mn<sub>3</sub>O<sub>4</sub> were synthesized by precipitation method. The size, morphology, and crystallinity of the resulting Mn<sub>3</sub>O<sub>4</sub>-NPs were investigated. In addition, *E. coli* and *S. aureus* bacterial strains were chosen to evaluate the vitro antimicrobial activity of Mn<sub>3</sub>O<sub>4</sub>-NPs using microdilution assay.

## MATERIALS AND METHODS

### Materials

Absolute ethanol, potassium permanganate KMnO<sub>4</sub>, monohydrate hydrazine N<sub>2</sub>H<sub>4</sub>.H<sub>2</sub>O, and sodium dodecylsulphate (SDS) were purchased from Merck Company.

### Synthesis of Mn<sub>3</sub>O<sub>4</sub> Nanoparticles

The starting materials used were 0.8 mmol of potassium permanganate (KMnO<sub>4</sub>) and 0.8 mmol of sodium dodecylsulphate which were dissolved in 40-ml distilled water. Then, 40 ml of an aqueous solution of monohydrate hydrazine (8 mmol) was added to the solution under magnetic stirring. The color of the prepared solution immediately turned from dark purple to black/brown then to orange/brown. The resulting solution was stirred for 1h at 70 °C and then was cooled down at room temperature. After that, the solution was separated *via* centrifugation. Finally, the solid was washed twice with distilled water and once more with ethanol and dried under vacuum environment.

### Characterization of Mn<sub>3</sub>O<sub>4</sub> Nanoparticles

The crystal structure of the powders was determined by XRD using a Bruker D8 Advance diffractometer (Ettlingen, Germany) with Cu K $\alpha$  radiation of wavelength 1.5405 Å in the range of 20° to 75°. The nanostructure morphology of the powders was observed by SEM using LEO 1450 VP system (Oberkochen, Germany). TEM (LEO 912AB) was also used for the estimation of crystalline structure,

morphology, and the average size of the prepared nanoparticles. FTIR spectrometer (Shimadzu4300, Nakagyo-ku, and Kyoto, Japan) was used to study the chemical bondings of the prepared samples.

## ANTIBACTERIAL TEST

The strains of *E. coli* ATCC25922 and *S. aureus* ATCC 25923 used in this study were subcultured from laboratory stocks. The antibacterial activity of the Mn<sub>3</sub>O<sub>4</sub>-NPs was tested against *E. coli* and *S. aureus* by determining the minimum inhibitory concentration (MIC) and minimal bactericidal concentration (MBC) using Broth Microdilution Method (according to the Clinical and Laboratory Standards Institute (CLSI) recommended MIC protocol with modifications) [14,15,16]. Bacteria were streaked from long-term storage at 85 °C in 15% glycerol stocks onto agar plates and incubated overnight at 37 °C. Colonies from the fresh plates were inoculated into Muller Hinton Broth (MHB) and grown at 37 °C in a shaking incubator at 200 rpm adjusted to 0.5 McFarland turbidity standards (10<sup>7</sup> cfu/ml). A stock solution of the Mn<sub>3</sub>O<sub>4</sub>-NPs was prepared in MHB medium. Mn<sub>3</sub>O<sub>4</sub> powder was sterilized under UV light before mixing with medium where no microbial growth observed in controls. Further serial of nanoparticles dilutions were made in the range of 1.25mg/ml to 39µg/ml. Then 70 µl of each diluted solution aliquot, 70 µl of MHB and inoculating 70 µl of the standardized microorganism suspensions were added to 96-well microplates (0.34 ml volume, Orange, Scientific). The microplates were then incubated at 37 °C for 48 h.

The MIC was the lowest concentrations at which each of the triplicate 96-well plate was clear after 0, 6, 12, 24 and 48 h of incubation. To evaluate MBC, a sample of 20 µl was transferred from each microtiter well without visible growth to a Muller Hinton plate and incubated at 37 °C for overnight. The MBC was the lowest concentration which could prevent the growth bacteria. The test was performed triplicate for each bacterium. Value that agreed on two or more occasions was adopted as the MIC or MBC of the strains.

Growth curves of *E. coli* and *S. aureus* exposed and unexposed to Mn<sub>3</sub>O<sub>4</sub>-NPs were determined by measuring absorbance at 630 nm by using an ELISA reader (Statfax-

2100, Awareness Technology Inc., USA). The percentage of growth inhibition (GI%) of each treatment at various reaction conditions was calculated in comparison with its own positive control using following equation:

$$\text{Percentage of growth inhibition (GI\%)} = \left( 100 - \frac{\text{OD}_{630} \text{ at the presence of antibacterial agent}}{\text{OD}_{630} \text{ at the absence of antibacterial agent}} \times 100 \right)$$

## RESULTS AND DISCUSSION

### Synthesis and Characterization

Figure 1 shows the XRD pattern of the synthesis of the  $\text{Mn}_3\text{O}_4$ -NPs. Diffracted peaks in the pattern are assigned to hausmannite phase, with  $I4_1/amd$  space group. This is in agreement with the previously published literature [5]. The additional small peaks seen in the pattern might be due to the formation of intermediate phases. As seen in Fig. 1, in addition to  $\text{Mn}_3\text{O}_4$ , two more structures, monoclinic and orthorhombic, are also observed corresponding to  $\text{Mn}_5\text{O}_8$  and  $\text{MnO}$ , respectively. Therefore, these structures are similar to Salavati-Niasari *et al.* results [17].

Average crystallite size of the particles was estimated from the Scherer equation and was found out to be about 22 nm. The morphology of  $\text{Mn}_3\text{O}_4$  nanoparticles, shown in Figs. 2a,b, indicates the agglomerate of the prepared nanoparticles using SEM, with rather uniform spherical shape. Their diameter varies between 60 and 100 nm. Elemental analysis of the  $\text{Mn}_3\text{O}_4$  nanoparticles was achieved from the EDX spectra, as presented in Fig. 3. The Mn element was observed at 0.6, 5.8 and 6.6 keV. The oxygen and gold elements, employed as the reference background, are at 0.6 and 1.5 keV, respectively [13].

The morphology and size distribution of the particles were further studied by TEM. Figure 4 is the TEM image of nanocrystals showing that the particles have nearly spherical shapes with the size distributions of 10-30 nm.

Figure 5 demonstrates the FTIR spectrum of  $\text{Mn}_3\text{O}_4$  nanoparticles, which shows five peaks at wavelengths from 0-900 nm, displaying three main bonds at 621.84, 495.85 and 454.1  $\text{cm}^{-1}$ . The bonds at 621.84 and 495.85  $\text{cm}^{-1}$  are

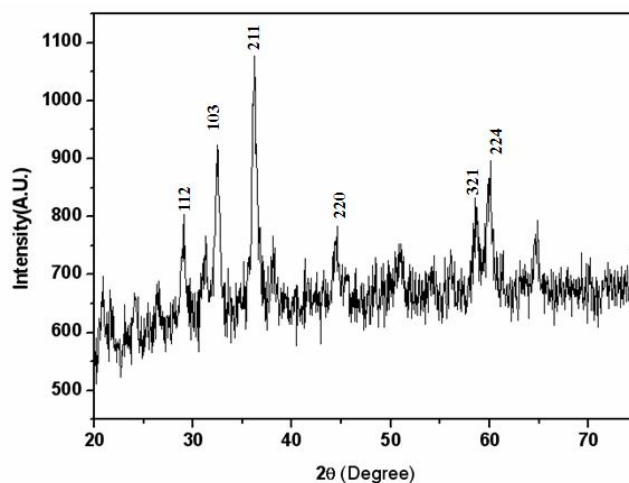


Fig. 1. XRD pattern of the  $\text{Mn}_3\text{O}_4$  nanopowders.

associated with the coupling of Mn-O stretching modes of tetrahedral and octahedral sites. The peak at 454.1  $\text{cm}^{-1}$  is related to the bond stretching mode of the octahedral site. Thus, these results confirm the formation of the composition in accordance with [18].

### Antibacterial Results

The antibacterial properties of  $\text{Mn}_3\text{O}_4$  nanoparticles against *E. coli* and *S. aureus* were examined by Broth Microdilution Method. Powder of  $\text{Mn}_3\text{O}_4$ -NPs was mixed with autoclaved MHB medium to make nanofluids with concentrations of 39, 78, 156, 312, 625 and 1250  $\mu\text{g ml}^{-1}$ . Figure 6 shows the inhibitory effect of these concentrations on the growth curve of the two representatives' bacteria from gram negative and gram positive groups, *E. coil* and *S. aureus*, respectively. As the value of the absorbance of the bacteria is increased, more light is being absorbed by bacteria. Results were calculated in the basis  $A/A_0$  in which A and  $A_0$  are final and initial absorbance measured by ELISA reader. Inhibitory effect of various concentrations of  $\text{Mn}_3\text{O}_4$ -NPs on *E. coil* growth increased when the amount of nanofluid concentration increased (Fig. 6a). As a consequence, clearly increase in bacteriostatic action of  $\text{Mn}_3\text{O}_4$ -NPs against *S. aureus* was observed at concentration of 312, 625 and 1250  $\mu\text{g ml}^{-1}$  during 48 h incubation at 37 °C (Fig. 6b). Furthermore inhibition of bacterial growth in these concentrations (312, 625 and 1250  $\mu\text{g ml}^{-1}$ ) were

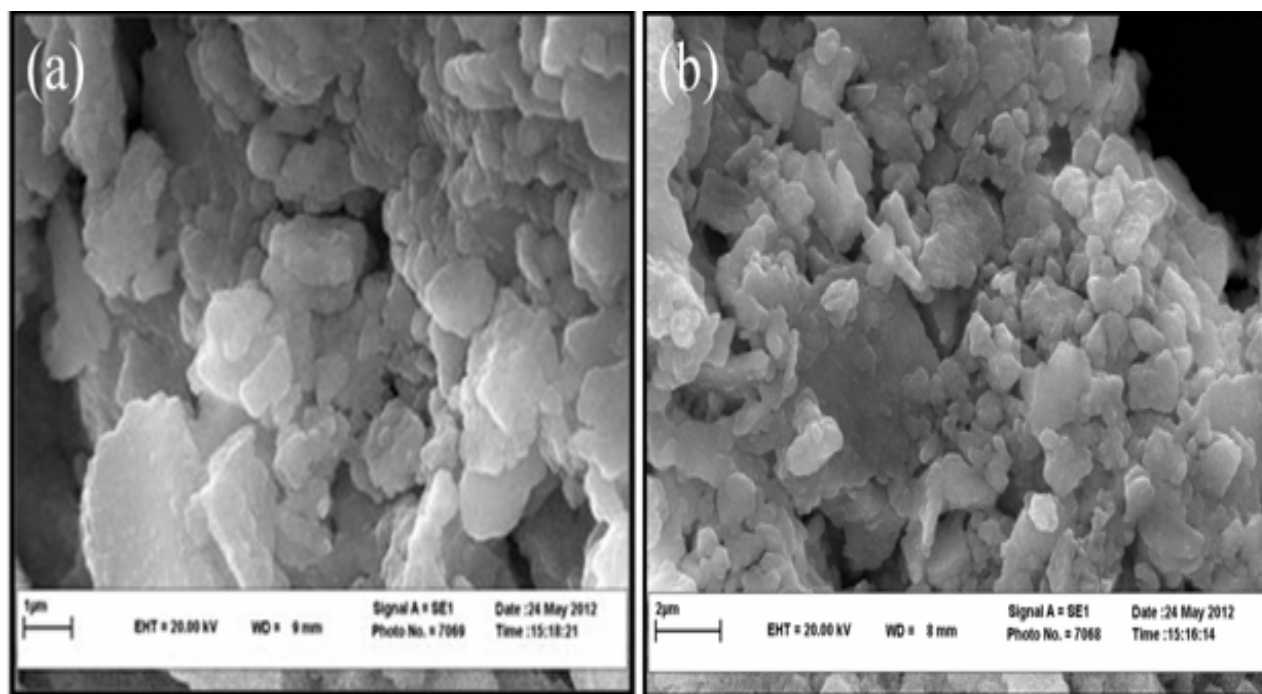


Fig. 2. SEM images of  $Mn_3O_4$ -NPs.

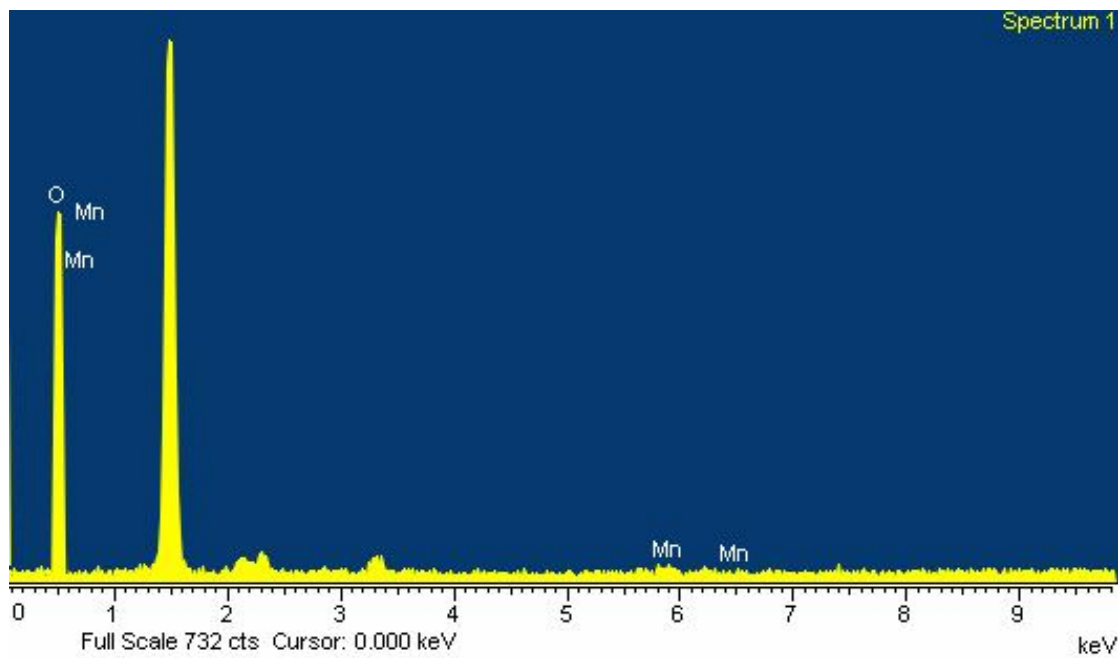
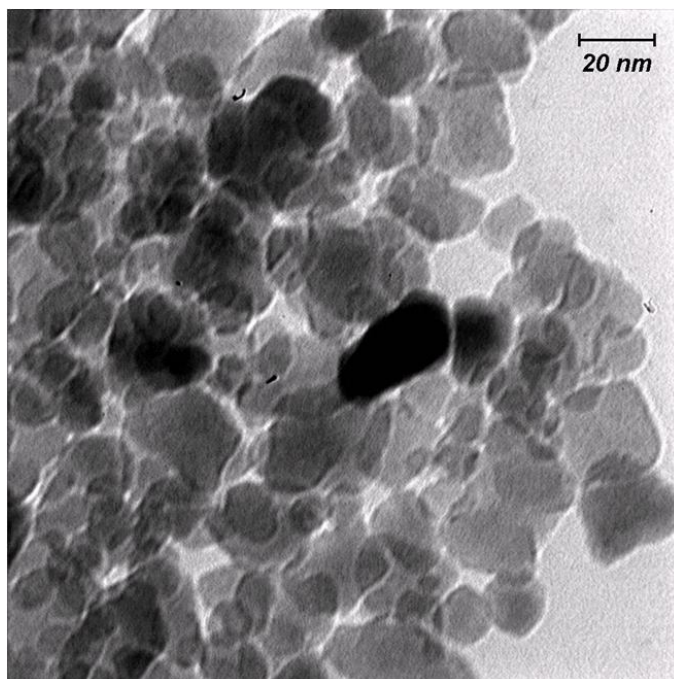
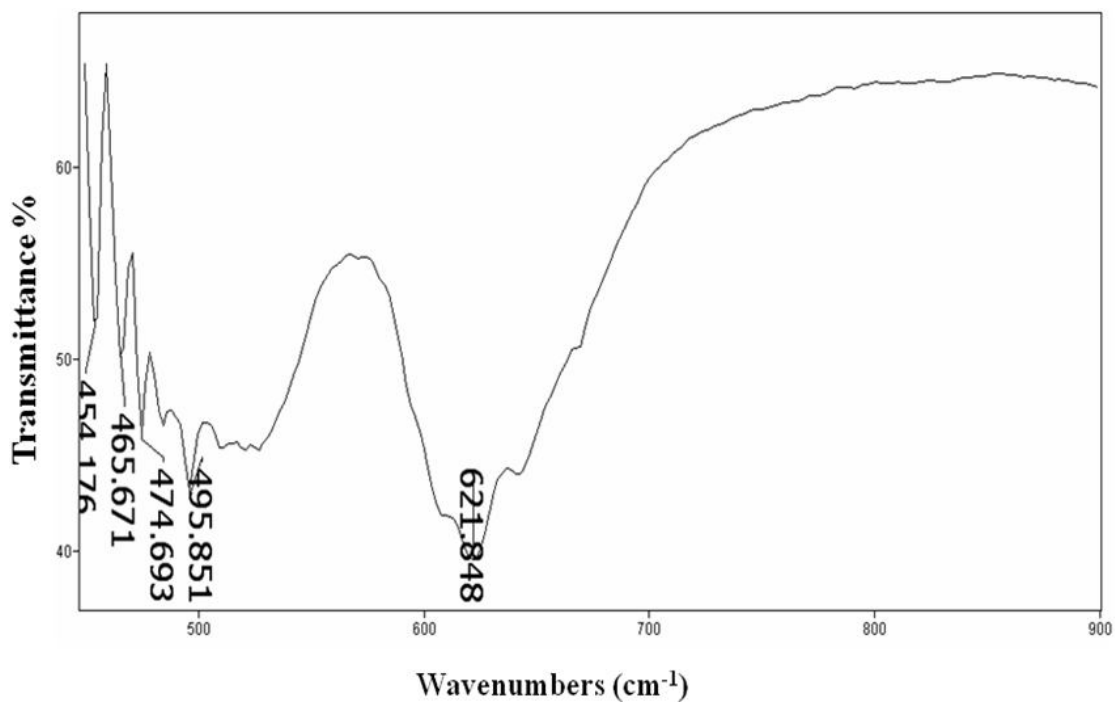


Fig. 3. EDX analysis of the  $Mn_3O_4$  nanopowders.



**Fig. 4.** TEM image of Mn<sub>3</sub>O<sub>4</sub>-NPs.



**Fig. 5.** FTIR spectrum of Mn<sub>3</sub>O<sub>4</sub>-NPs.

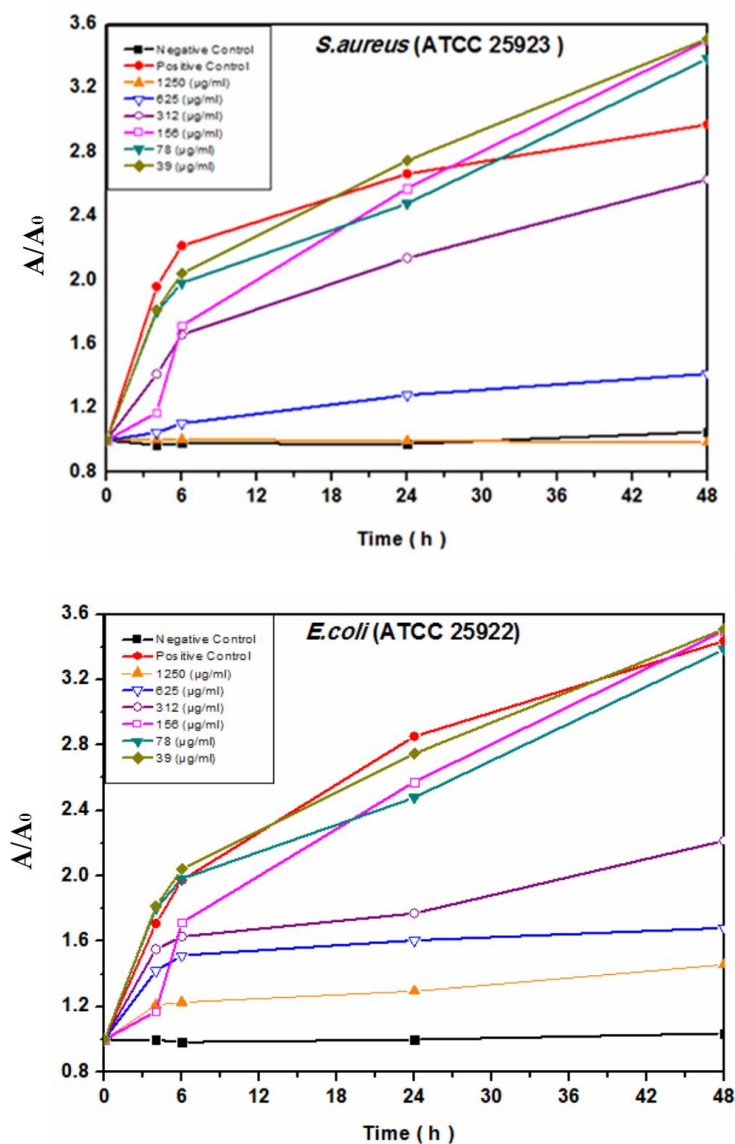


**Fig. 6.** Growth curves of *E. coli* and *S. aureus* in MHB medium inoculated with  $10^7$  cfu ml<sup>-1</sup> of bacteria (a) *E. coli* and (b) *S. aureus* in the presence of six different concentrations of Mn<sub>3</sub>O<sub>4</sub>-NPs.

about 43, 93 and 100% for *S. aureus* while for *E. coli* were 66, 68 and 78%, respectively, (Fig. 7) indicating that percentage of growth inhibition for *E. coli* was higher in low concentration, while for *S. aureus* was more in higher concentrations. Antibacterial activity of nanoparticles mostly correlates with their concentration and size as shown by many studies. Kim *et al.* (2007) [19] used various concentrations of silver nanoparticles and demonstrated the decrease of activity with the decrease of concentration

against *E. coli* and *S. aureus*. They found that lower concentrations of NPs were significantly less effective for *E. coli* whereas against *S. aureus* all tested concentrations showed less effectiveness, however a general tendency of decreasing activity with decreased concentration was still present.

The MIC and MBC values for Mn<sub>3</sub>O<sub>4</sub>-NPs were determined and shown in Table 1. MIC results showed that gram negative bacteria (*E. coli*) were more sensitive to

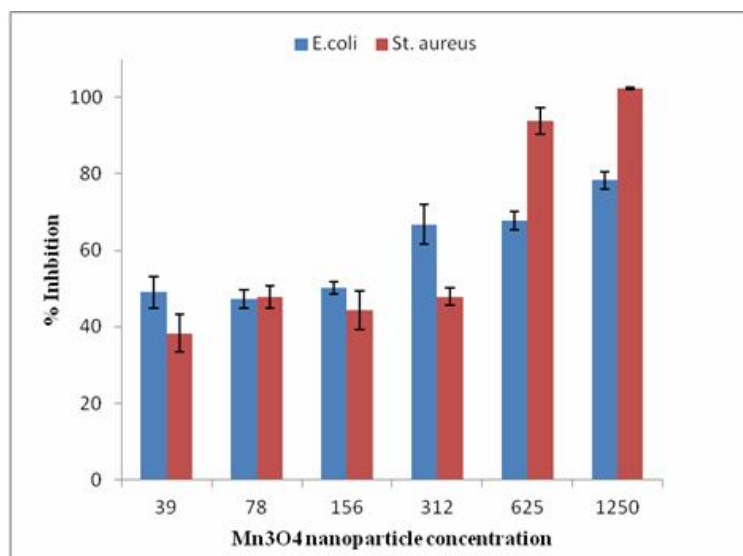


**Fig. 7.** Percentage of bacterial growth inhibition at different Mn<sub>3</sub>O<sub>4</sub> -NPs-NPs.

**Table 1.** Minimum Inhibitory Concentration (MIC) and Minimal Bactericidal Concentration (MBC) of Mn<sub>3</sub>O<sub>4</sub> -NPs against *E. coli* and *S. aureus* ( $\mu\text{g ml}^{-1}$ )

Bacterial	MIC ( $\mu\text{g ml}^{-1}$ )	MBC ( $\mu\text{g ml}^{-1}$ )
<i>E. coli</i> (ATCC 25922)	312	>1250
<i>S. aureus</i> (ATCC 25923)	625	1250

Mn<sub>3</sub>O<sub>4</sub>-NPs than gram positive bacteria (*S. aureus*). It was probably resulted from the different characteristics of the bacterial cell surfaces and its interaction with nanoparticles [20]. This finding could be more or less extended to Mn<sub>3</sub>O<sub>4</sub>-NPs damage effects on membrane wall of the bacteria, however more investigation is needed [21].

However, the exact antibacterial mechanism of Mn<sub>3</sub>O<sub>4</sub> nanoparticles has not been clearly revealed yet. There is a well-documented link between metal oxide NPs such as ZnO and oxidative stress (Zhang *et al.* 2008; Ma *et al.* 2012; Shi *et al.*, 2014) [22-24]; one of the possible modes that can

be suggested for Mn<sub>3</sub>O<sub>4</sub> NPs may be the production of reactive oxygen species (ROS). ROS can be produced when metal oxide NPs powder such as ZnO is suspended in water, disrupting the cell membrane acting as bactericidal agent (Lipovsky *et al.* 2009; Gondal *et al.* 2011; Raghpati 2012) [25,26].

## CONCLUSIONS

Mn<sub>3</sub>O<sub>4</sub>-NPs were prepared *via* reduction method and characterized by XRD, SEM, TEM and FTIR. XRD pattern

shows that the dominant hausmannite phase is  $Mn_3O_4$ . SEM images show that  $Mn_3O_4$  nanoparticles have agglomerated but are not uniform, and their size varies between 60 and 100 nm. The chemical composition of  $Mn_3O_4$  nanoparticles was investigated by EDX technique, which revealed the presence of Mn and O elements. TEM image shows that the particle shapes are nearly spherical with the size of 10 to 30 nm. Analyzing the FTIR spectrum revealed the presence of Mn-O bonds and hydroxyl groups.  $Mn_3O_4$ -NPs were found to have antibacterial activity against *E. coli* and *S. aureus*. The inhibitory effects increase as the concentration of  $Mn_3O_4$ -NPs is increased. According to MIC results,  $Mn_3O_4$ -NPs have well potential for various antibacterial applications. The effect of the  $Mn_3O_4$ -NPs was found to be significantly more pronounced on *E. coli* compared with *S. aureus* bacterial.

## REFERENCES

- [1] D.P. Dubal, D.S. Dhawale, R.R. Salunkhe, V.J. Fulari, C.D. Lokhande, *Alloys and Compounds* 497 (2010) 166. A. Olmos, R. Redon, G. Gattorno, M.E. Zamora, F. Leal, A. Osorio, *Colloid and Interface Sci.* 291 (2005) 175.
- [2] A.R. Armstrong, P.G. Bruce, *Nature* 381 (1996) 499.
- [3] A. Moses Ezhil Raj, S.G. Victoria, V.B. Jothy, C. Ravidhas, J. Wollschläger, M. Suendorf, M. Neumann, M. Jayachandran, C. Sanjeeviraja, *Appl. Surf. Sci.* 256 (2010) 2920.
- [4] L. Laffont, P. Gibot, *Mater. Charact.* 61 (2010) 1268.
- [5] Y.Q. Chang, X.Y. Xu, X.H. Luo, C.P. Chen, D.P. Yu, *J. Cryst. Growth* 264 (2004) 232.
- [6] A. Olmos, R. Redon, M.E. Zamora, F. Leal, A. Osorio, J.M. Saniger, *Rev. Adv. Mater. Sci.* 10 (2005) 362.
- [7] Z. Chen, J.K.L. Lai, C.H. Shek, *J. Chem. Phys.* 124 (2006) 184707.
- [8] Y. Yamashita, K. Mukai, J. Yoshinobu, M. Lippmaa, T. Kinoshita, M. Kawasaki, *Surf. Sci.* 514 (2002) 54.
- [9] T. Ahmad, K.V. Ramanujachary, S.E. Lofland, A.K. Ganguli, *Mater. Chem.* 14 (2004) 3406.
- [10] F. Jiao, A. Harrison, A.H. Hill, P.G. Bruce, *Adv. Mater.* 19 (2007) 4063.
- [11] M.J. Hajipour, K.M. Fromm, A.A. Ashkarran, D.J. Aberasturi, I.R. Larramendi, T. Rojo, V. Serpooshan, W.J. Parak, M. Mahmoudi, *Trends Biotechnol.* 30 (2012) 499.
- [12] C. Al-Nakib, A. Shafiul, A. Aktaruzzaman, R. Abdur, *J. Hazard. Mater.* 172 (2009) 1229.
- [13] Clinical and Laboratory Standards Institute, *Approved Standard-Eighth Edition Approved Standard M11-A8, 2012*, Villanova, PA, USA.
- [14] Clinical and Laboratory Standards Institute, *third Informational Supplement*. Wayne (Penn): CLSI; *Approved Standard M27-A*; 1997.
- [15] Clinical and Laboratory Standards Institute, Wayne (Penn): CLSI; 2003.
- [16] M. Salavati-Niasari, F. Davar, M. Mazaheri, *Polyhedron* 27 (2008) 3467.
- [17] A. Baykal, Y. Koseoglu, M. Senel, *CEJC.* 5 (2007) 169.
- [18] K. Kevin, S. Young. W.C. Richard, *RNA* 13 (2007) 22.
- [19] P.K. Stoimenov, R.L. Klinger, G.L. Marchin, K.J. Klabunde, *Langmuir* 18 (2002) 6679.
- [20] L.L. Zhang, Y.H. Jiang, Y.L. Ding, M. Povey, D. York, *Nanopart. Res.* 9 (2007) 479.
- [21] L. Zhang, Y. Ding, M. Povey, D. York, *Prog. Nat. Sci.* 18 (2008) 939.
- [22] J. Ma, J. Liu, Y. Bao, Z. Zhu, X. Wang, J. Zhang, *Ceram Int.* 39 (2012) 2803.
- [23] L.-E. Shi, Z.-H. Li, Z. Wei, Y.-F. Zhao, Y.-F. Jin, Z.-X. Tang, *Food Additives & Contaminants: Part A*, 2014: DOI: 10.1080/19440049.2013.865147.
- [24] A. Lipovsky, Z. Tzitrinovich, H. Friedmann, G. Applerot, A. Gedanken, R. Lubart, *Phys. Chem. C* 113 (2009) 15997.
- [25] R.K. Raghupati, R.T. Koodali, A.C. Manna, *Langmuir* 27 (2011) 4020.